Immunity
Resource

Functional Analysis via Standardized Whole-Blood Stimulation Systems Defines the Boundaries of a Healthy Immune Response to Complex Stimuli

Darragh Duffy,[1,2,3,14] Vincent Rouilly,[1,4,14] Valentina Libri,[1,14] Milena Hasan,[1] Benoit Beitz,[1] Mikael David,[1] Alejandra Urrutia,[1,2,3] Aurélie Bisiaux,[2,3] Samuel T. LaBrie,[5] Annick Dubois,[6] Ivo G. Boneca,[7,8] Cécile Delval,[6] Stéphanie Thomas,[1,2,3] Lars Rogge,[1,9] Manfred Schmolz,[10] Lluis Quintana-Murci,[11,12,15,*] and Matthew L. Albert[1,2,3,13,15,*] for The *Milieu Intérieur* Consortium

[1]Center for Human Immunology, Institut Pasteur, 75015 Paris, France
[2]INSERM U818, 75015 Paris, France
[3]Laboratory of Dendritic Cell Immunobiology, Department of Immunology, Institut Pasteur, 75015 Paris, France
[4]Center for Bioinformatics, Institut Pasteur, 75015 Paris, France
[5]Myriad Rules Based Medicine, Inc., Austin, TX 78759, USA
[6]Center for the Integration of Clinical Research, Institut Pasteur, 75015 Paris, France
[7]Laboratory of Biology & Genetics of the Bacterial Cell Wall, Department of Microbiology, Institut Pasteur, 75015 Paris, France
[8]INSERM, Equipe Avenir, 75015 Paris, France
[9]Laboratory of Immunoregulation, Department of Immunology, Institut Pasteur, 75015 Paris, France
[10]Myriad Rules Based Medicine, Inc., 72770 Reutlingen, Germany
[11]Laboratory of Human Evolutionary Genetics, Department of Genomes & Genetics, Institut Pasteur, 75015 Paris, France
[12]CNRS URA3012, 75015 Paris, France
[13]INSERM UMS20, 75015 Paris, France
[14]These authors contributed equally to this work
[15]These authors contributed equally to this work
*Correspondence: quintana@pasteur.fr (L.Q.-M.), albertm@pasteur.fr (M.L.A.)
http://dx.doi.org/10.1016/j.immuni.2014.03.002

SUMMARY

Standardization of immunophenotyping procedures has become a high priority. We have developed a suite of whole-blood, syringe-based assay systems that can be used to reproducibly assess induced innate or adaptive immune responses. By eliminating preanalytical errors associated with immune monitoring, we have defined the protein signatures induced by (1) medically relevant bacteria, fungi, and viruses; (2) agonists specific for defined host sensors; (3) clinically employed cytokines; and (4) activators of T cell immunity. Our results provide an initial assessment of healthy donor reference values for induced cytokines and chemokines and we report the failure to release interleukin-1α as a common immunological phenotype. The observed naturally occurring variation of the immune response may help to explain differential susceptibility to disease or response to therapeutic intervention. The implementation of a general solution for assessment of functional immune responses will help support harmonization of clinical studies and data sharing.

INTRODUCTION

The immune system is responsible for maintaining a healthy state, ensuring beneficial cohabitation with microbiota, and preventing infection. Immune system dysfunction is often associated with increased susceptibility to infection, inflammation, autoimmunity, or even development of cancer. Moreover, individual heterogeneity in the immune response can have important medical consequences, such as the likelihood to respond to anti-infectious therapy, the efficiency of vaccine administration, or the development of side effects secondary to treatment. Because of the complexity of immune responses at both the individual and population level, it has not been possible, thus far, to define the boundaries of a "healthy immune response" or its naturally occurring variability. Most studies have taken a disease-based approach, from which considerable insight into immune mechanisms has been obtained. Nonetheless, to utilize this information in diagnosis and disease management, the assessment of a healthy functional immune response within the human population is required. Specifically, there is an unmet need for reliable and reproducible assay systems for studying human immune responsiveness. In other words, we must overcome technical challenges and preanalytical error in order to assess the true variability in functional immune responses. Only then will immunologists be positioned to contribute to the promises of personalized medicine, applying simple-to-use technologies that provide in-depth understanding of the phenotypic variance of immune responses in the human population.

Human innate or adaptive immune responsiveness is typically studied in vitro, thereby permitting the evaluation of multiple stimulation conditions in parallel. Standard laboratory practice is to transport collected blood to a centralized facility, thereby allowing isolation of peripheral blood mononuclear cells (PBMCs) by Ficoll-Hypaque gradient centrifugation by trained

personnel (Folds and Schmitz, 2003). Stimulation can be performed immediately, but often cells are cryopreserved in order to batch test samples (Maecker et al., 2012). In addition to this process being labor intensive, there is a risk of sample contamination by microbial components (e.g., bacterial endotoxin). Moreover, sample handling results in variable loss of cells and cryopreservation diminishes functional responsiveness, also in a nonlinear and/or nonreproducible way (Chen et al., 2010). Although whole-blood human lymphocyte assays were first innovated in 1975 (Eskola et al., 1975), they have not been widely used in scientific research or clinical evaluation of functional immune responses. Notably, direct measurements made in whole blood have the advantages of minimizing contamination and sample handling. Moreover, maintaining total leukocytes (e.g., polymorphonuclear cells) and platelets in a plasma matrix may provide a more accurate reflection of natural responsiveness to immune stimuli (Chen et al., 2010; De Groote et al., 1992; Ida et al., 2006; Kirchner et al., 1982; Schmolz et al., 2004).

Herein, we report the development of 27 whole-blood stimulation systems, built into syringe-based medical devices that may be utilized in point-of-care approaches and tested in 25 ethnically well-defined individuals of European ancestry. With these stimulation conditions, we define the boundaries of a healthy immune response to complex stimuli (i.e., whole microbes), including gram-negative bacteria, gram-positive bacteria, mycobacteria, fungi, and live viruses (Krishna and Miller, 2012; Miettinen et al., 2008; Stuyt et al., 2003; Stuyt et al., 2001; Zhao et al., 2007). In addition, we developed assay systems to study the response to purified or synthetic ligands for the major innate host response pathways, including those triggered by the Toll-like receptors (TLRs) (Alexopoulou et al., 2001; Diebold et al., 2004; Gantner et al., 2003; Godaly and Young, 2005; Hayashi et al., 2001; Hemmi et al., 2000, 2002; Jurk et al., 2002; Liu-Bryan et al., 2005; Takeuchi et al., 1999; Zhao et al., 2007), nucleotide-binding domain and leucine-rich repeat containing molecules (NLRs) (Allen et al., 2009; Ichinohe et al., 2009), and C-type lectin-like receptors (CLRs) (Brown et al., 2003). To directly evaluate the variable responses after cytokine receptor signaling, we also tested several clinically employed cytokines such as interferon-alpha (IFN-α), interferon-beta (IFN-β), interferon-gamma (IFN-γ), tumor necrosis factor-alpha (TNF-α), interleukin 1-beta (IL-1β), and interleukin 23 (IL-23) (Dinarello, 2012; González-Navajas et al., 2012; Oppmann et al., 2000; Platanias, 2005; Zheng et al., 2013). Finally, we utilized direct T cell receptor cross-linking (anti-CD3+anti-CD28) and super-antigen stimulation as two distinct mechanisms for eliciting T cell activation (Smith-Garvin et al., 2009). By quantifying the stimulus-induced production of cytokines, chemokines, and growth factors, it was possible to establish specific protein signatures for each stimulation system and we establish reference values as well as an estimate of variation among healthy individuals originating from a homogeneous ethnic background. These tools and the data set provided will be a valuable resource for the immunologic community. Moreover, we propose that through coordinated use of validated assay systems and open sharing of data sets, it will be possible to rapidly implement measures of functional immune responsiveness into clinical studies and medical practice.

RESULTS

Reproducible Whole-Blood Assays for Assessing Innate and Adaptive Immune Responses

To establish in vitro assay systems that preserve physiological cellular interactions, we developed syringe-based medical devices that can be used for activating immune cells present in whole blood. Fifty-four stimuli were considered for study and evaluated for sterility, solubility, dose response, short and long-term stability, and reproducibility (exclusion criteria are detailed in Supplemental Experimental Procedures available online). Based on initial testing, we prioritized 27 stimuli for development in TruCulture whole-blood collection and culture devices (Myraid RBM) (Table 1). In brief, during the manufacturing process (certified according to ISO 13845) of the TruCulture collection syringes, the indicated stimuli were dissolved in the proprietary TruCulture cell medium (2 ml per tube). These TruCulture systems were then frozen and stored at -20°C until use. After thawing to room temperature, the collection syringes were filled with 1 ml whole blood and incubated for 22 hr ($\pm$10 min) in room air at 37°C ($\pm$1°C), utilizing a bench-top heating block (VLMH GmbH). After immune stimulation, insertion of a valve separator (an integral part of the TruCulture system) yielded a culture supernatant that was aliquoted and stored at -80°C for subsequent multiplex protein immunoassay testing (Figure S1A).

For all stimuli, we selected low and highly induced protein analytes that could be measured and used for dose-finding studies. We selected dose concentrations for the stimuli that maximized the ability to detect low-expressed proteins, while taking precautions not to exceed the upper limit of the biologic range for highly expressed proteins. Representative data for one microbe, MAMP, and T cell stimulus is shown (Figure S1B), and the selected dose for all assays can be found in Table 1. We further validated our assay systems by serially testing individual responsiveness to immune stimulation, repeating the measurements four times at the same time point (Figure S1C) and four times over a 25-day time period (Figure S1D). As represented by the data of lipopolysaccharide (LPS)-induced responses, 25 of the 27 stimuli induced protein signatures with intraindividual coefficients of variance (CVs) ranging from 5 to 14 (Figure 1D, Table S1, and data not shown). The two exceptions were calcium pyrophosphate dihydrate crystals (CPPD) and whole glutan particles (WGPs), both of which are particulate agonists that were difficult to homogenize in liquid suspension and resulted in higher technical variation (Table S1). Regarding the response to LPS (Figure S1D), substantial variability could be observed among the three donors tested. Donor G showed high levels of IL-6 but intermediate induction of IFN-γ. By contrast, donor H showed the highest production of IFN-γ but the lowest induction of IL-6. Additional quality-control data, including selection of anticoagulant used, can be found in the Supplemental Experimental Procedures and Table S2.

Quantitative and Qualitative Differences in Healthy Donor Responses to Immune Stimulation

To demonstrate the utility of our whole-blood stimulation systems, we recruited 25 healthy volunteers of European ancestry, aged 30–39 and stratified by gender (13 women, 12 men).

Table 1. Innate and Adaptive Immune Stimuli Used for Development of Whole-Blood Stimulation Systems

Stimulus	Abbreviation	Concentration	Supplier	Sensor or Receptor	Reference
Null	Ø		NA		
Microbe					
HK *E. coli 0111:B4*	HKEC	10^7 bacteria	Invivogen	complex	Takeuchi et al., 1999
HK *S. aureus*	HKSA	10^7 bacteria	Invivogen	complex	Krishna and Miller, 2012
HK *L. rhamnosus*	HKLR	10^7 bacteria	Invivogen	complex	Miettinen et al., 2008
BCG (Immucyst)	BCG	3×10^5 bacteria	Sanofi Pasteur	complex	Means et al., 1999; Godaly and Young, 2005; Randhawa et al., 2011
HK *H. pylori*	HKHP	10^7 bacteria	Invivogen	complex	Zhao et al., 2007
HK *C. albicans*	HKCA	10^7 bacteria	Invivogen	complex	Brown et al., 2003; Gantner et al., 2003
Influenza A virus (live)	IAV	100 HAU	Charles Rivers	complex	Diebold et al., 2004; Kato et al., 2006; Ichinohe et al., 2009; Allen et al., 2009
Sendai virus (live)	SeV	10 HAU	Charles Rivers	Rig-I and Mda/5	Yoneyama et al., 2005; Kato et al., 2005
MAMP					
C12-iE-DAP	DAP	4 μg/ml	Invivogen	NOD1	Chamaillard et al., 2003
CPPD	CPPD	100 μg/ml	Invivogen	NLRP3 and TLR2	Liu-Bryan et al., 2005; Martinon et al., 2006
FSL-1	FSL	2 μg/ml	Invivogen	TLR2/6	Shibata et al., 1997; Okusawa et al., 2004
Poly I:C	pIC	20 μg/ml	Invivogen	TLR3	Alexopoulou et al., 2001
LPS-EB (ultrapure)	LPS	10 ng/ml	Invivogen	TLR4	Poltorak et al., 1998; Shimazu et al., 1999
Flagellin-ST	FLA	0.25 μg/ml	Invivogen	TLR5	Hayashi et al., 2001
Gardiquimod	GARD	3 μM	Invivogen	TLR7	Hemmi et al., 2002
R848	R848	1 μM	Invivogen	TLR7 and TLR8	Jurk et al., 2002
ODN 2216	ODN	25 μg/ml	Invivogen	TLR9	Hemmi et al., 2000; Krieg, 2002
lipoarabinomannan	LAM	10 μg/ml	Invivogen	Mannose R, CD36	Józefowski et al., 2011; Sieling et al., 1995
WGP	WPG	40 μg/ml	Invivogen	Dectin-1	Goodridge et al, 2011
Cytokines					
IFN-α_{2b} (Intron A)	IFN-A	1,000 IU/ml	Merck	IFNAR	González-Navajas et al., 2012
IFN-β (Betaseron)	IFN-B	1,000 IU/ml	Bayer	IFNAR	González-Navajas et al., 2012
IFN-γ (Imukin)	IFN-G	1,000 IU/ml	Boehringer Ingelheim	IFNγR	Platanias, 2005
TNF-α	TNF-A	10 ng/ml	Miltenyi Biotech	TNFR	Kolb and Granger, 1968
IL-1β	IL-1B	25 ng/ml	Peprotec	IL1R	March et al., 1985
IL-23	IL-23	50 ng/ml	Miltenyi Biotech	IL23R	Oppmann et al., 2000
T Cells					
α-CD3 + α-CD28	CD3+CD28	0.4 μg/ml + 0.33 μg/ml	RND Systems + Beckman Coulter	TCR	Smith-Garvin et al., 2009
Enterotoxin SEB	SEB	0.4 μg/ml	Bernhard Nocht Institute	TCR and MHC II	Fleischer and Schrezenmeier, 1988

Abbreviations are as follows: HK, heat killed; HAU, hemagglutanin units; IU, international units.
The 28 stimulation conditions used for the preparation of TruCulture tubes are listed, with the indicated dose and commercial supplier. Stimuli are ordered based on four categories: whole microbe, MAMP, cytokine, and T cell agonist. See also Figure S1 and Tables S1, S2, S3, and S4.

Samples were collected, processed, and analyzed as described (Figure S1A). Luminex assays employed in the study are listed and the lower limit of quantification (LLOQ) and least detectable doses (LLD) for each assay are indicated (Table S3). In order to assess the overall signatures induced in the 28 conditions, we plotted the concentration of the measured analytes across all donors (four representative stimulation systems are shown: HKEC, LPS, IL-1β, and CD3+CD28, with the null response overlayed in each graph; Figure 1). Notably, we achieved a range of induced biologic responses, spanning, in some instances, greater than 1,000-fold as compared to the null condition (e.g., IL-6, MIP-1α). Importantly, the stimulations achieved by the assay systems did not exceed the measured biologic limit (as defined by a plateau in the response of selected analytes), and a broad range of induced protein responses were observed. Several protein analytes remained unchanged across all stimulation systems (i.e., IL-7, MMP-3, and sICAM-1) and were therefore removed from further analysis.

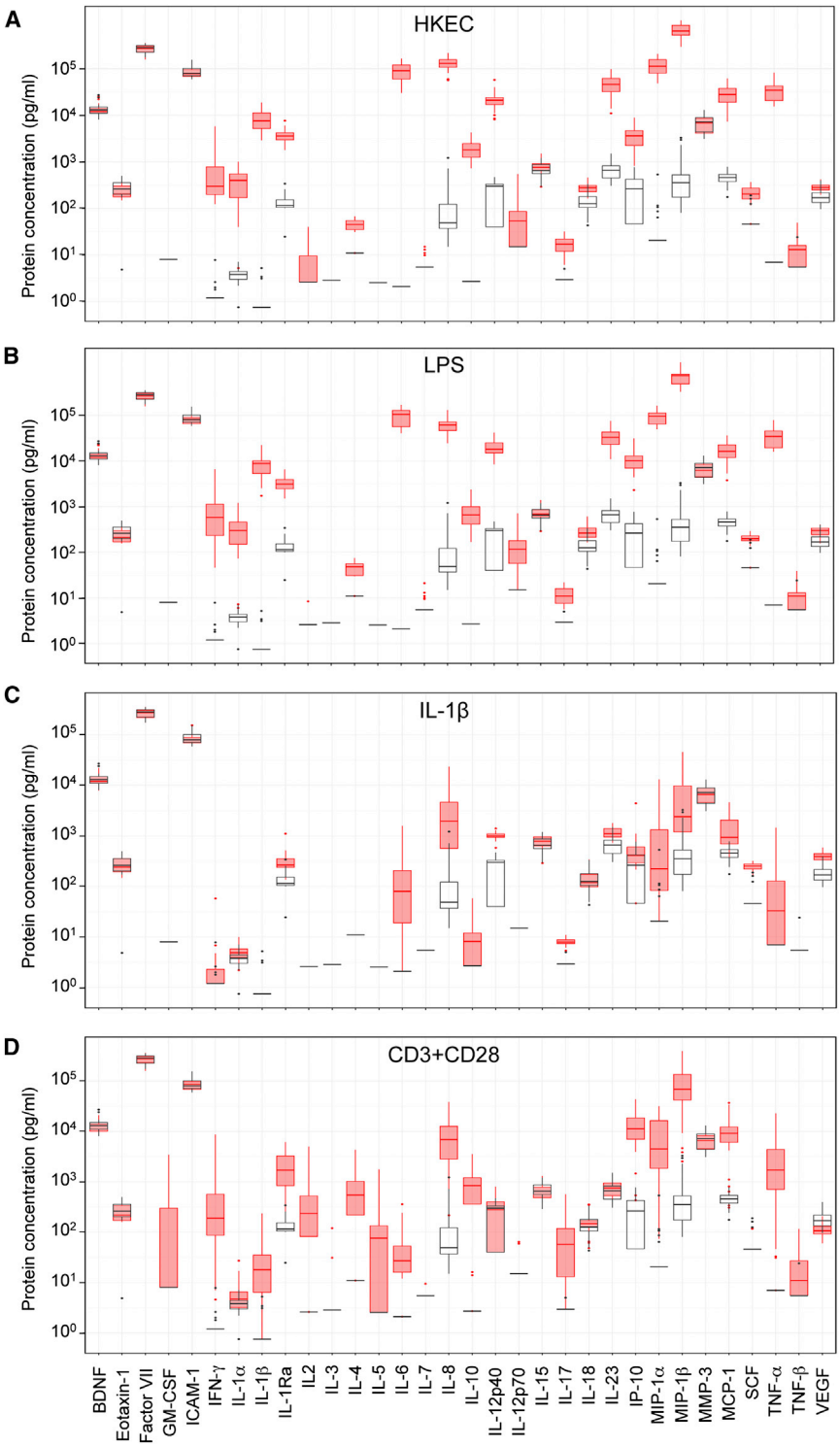

Figure 1. Dynamic Range of Stimulation Systems

Box-whisker plots indicate the induced protein response for 25 healthy donors for 4 representative stimuli: HKEC (A), LPS (B), IL-1β (C), and CD3+CD28 (D). Induced responses are in red, and the null response is overlaid in gray. Protein analytes are reported in pg/ml and listed alphabetically. The median is represented by the horizontal line, the interquartile range (IQR) by the box, and the whiskers represent 1.5 × IQR. Data beyond the end of the whiskers are outliers and plotted as points.

We next analyzed the data by unsupervised principal component analysis (PCA), employing Qlucore Omics Explorer 2.3 (Andersson et al., 2005). Prior to applying PCA, values for each of the 29 protein analytes were centered to a mean value of zero and scaled to unit variance. The 27 stimuli and null control are indicated by the filled circles and the vector position of each of the 25 donors is represented (Figure 2A). The PCA revealed strong stimuli-specific clusters, with the first three principal component (PC) vectors explaining 57% of the total variance (Figures 2A and 2B). Highlighting the presence of a common, core signature for the induced innate response, we found that PC1 is composed by the contribution of chemokines and cytokines: MIP-1α, MIP-1β, TNF-α, IL-6, IL-8, IL-10, IL-1RA, and MCP-1. Interestingly, PC2 separated stimuli that induced an adaptive immune signature and was mainly driven by IL-5, IL-2, GM-CSF, and IL-4. Stimuli that were directed toward the second principal component axis included CD3+CD28, SEB, and to a lesser extent *Candida albicans* (HKCA), bacillus Calmette-Guerin (BCG), and *Staphylococcus aureus* (HKSA). PC3 was composed of IL-12p70 and IP-10 as induced analytes and Factor-VII as a suppressed factor. The signature achieved by pIC stimulation could be easily separated across this third principal component axis. Illustrating how the calculated vectors relate to the overall PCA, we superimposed expression data for the top analyte of each vector on the PCA plot (Figure 2C).

To further validate our approach and to explore the underlying architecture of the PCA, we focused on the two T cell stimulation systems: CD3+CD28 and SEB stimulation. When analyzed separately, the two stimulation conditions could be easily distinguished with a PCA plot that was based on 12 protein analytes that showed statistical differences (CD3+CD28 versus SEB, MW q value < 0.05) (Figures 3A–3C Interestingly, CD3+CD28 and SEB induced similar amounts of T cell cytokines (e.g., IL-4, IL-5); however, the distinct mechanisms of activation—unique action on the TCR signaling pathway as compared to cross-linking of MHCII and the TCR, respectively (Fleischer and Schrezenmeier, 1988)—accounted for higher

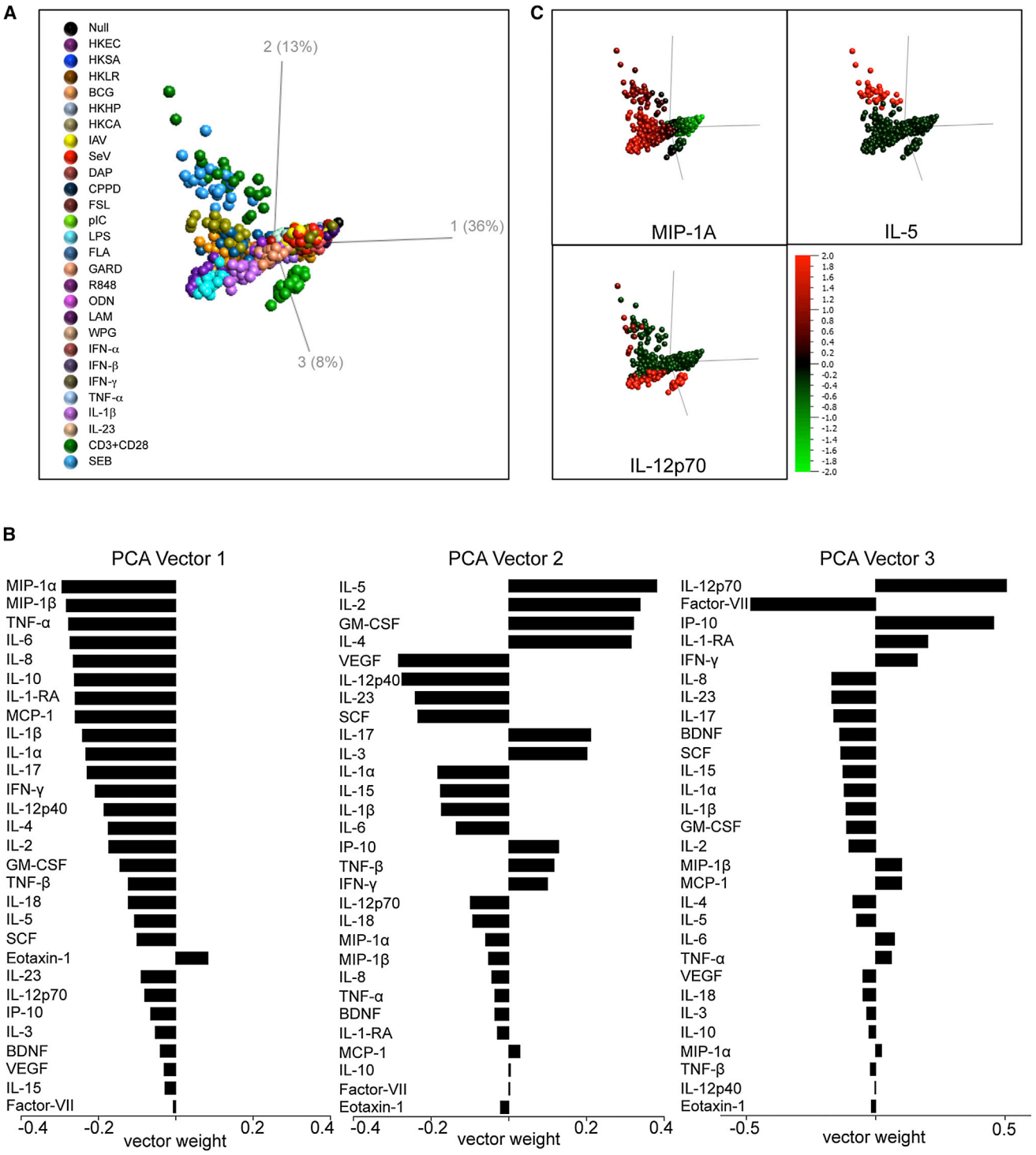

Figure 2. Distinct Inflammatory Signatures for Stimulation Systems

(A) Principal component analysis (PCA) was performed on the data set obtained from 25 healthy donors. Each colored circle represents one of the 28 different whole-blood stimulation conditions, and the PCA was run with data obtained from the analysis of 29 proteins. The PCA plot shown captures 57% of the total variance within the selected data set (PCA1, 36%; PCA2, 13%; PCA3, 8%).

(B) The contribution of each protein analyte to the three principal component axes of the PCA plot are shown. (The positioning of the bars is arbitrary and is not considered negative or positive except in relation to the other analytes.)

(C) The protein analyte contributing most strongly to each of the three principal component axes was overlaid on the PCA plot. A heat map indicates the relative expression of the indicated protein analyte (red indicating high levels of expression, green indicating low levels of expression).

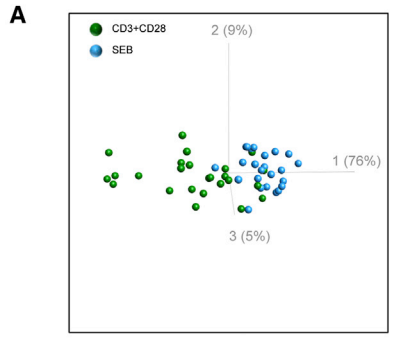

B

Analyte	p value	q value
IL-6	$3.78x10^{-14}$	$1.18x10^{-12}$
IL-8	$4.08x10^{-11}$	$6.53x10^{-10}$
MCP-1	$2.04x10^{-11}$	$2.179x10^{-9}$
IL-1β	$5.26x10^{-8}$	$4.21x10^{-8}$
IL-2	$2.75x10^{-8}$	$1.76x10^{-7}$
IL-17	$4.76x10^{-5}$	$2.53x10^{-4}$
GM-CSF	$1.0x10^{-4}$	$4.58x10^{-4}$
MIP-1α	$1.52x10^{-4}$	$6.08x10^{-4}$
IFN-γ	$1.8x10^{-4}$	$6.51x10^{-4}$
TNF-α	$6.4x10^{-4}$	$2.06x10^{-3}$
IL-1α	$1.42x10^{-3}$	$4.13x10^{-3}$
IL-15	$1.38x10^{-2}$	$3.68x10^{-2}$

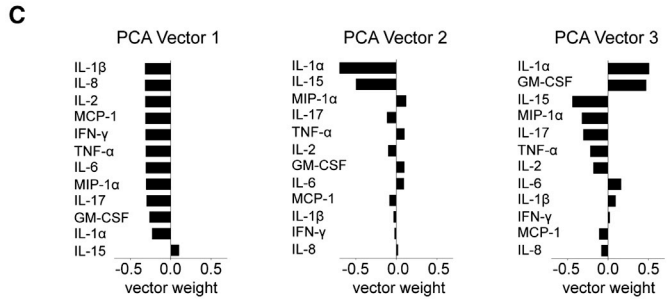

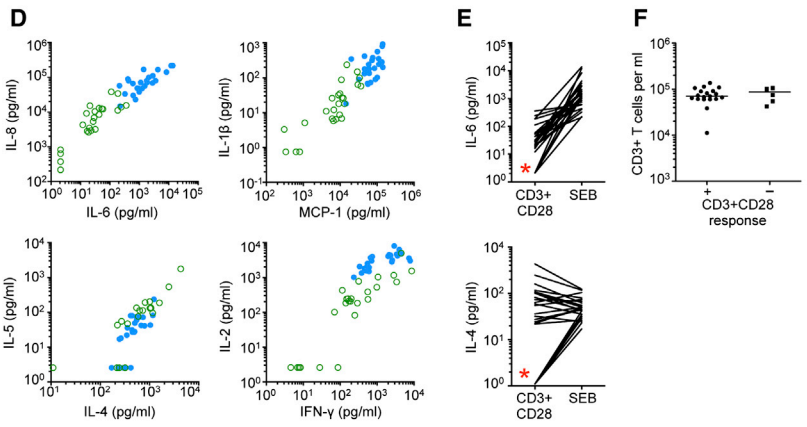

Figure 3. CD3+CD28 and SEB Induce Distinct Inflammatory Signatures

(A) Principal component analysis (PCA) was performed on the data set obtained from 25 healthy donors for the response to CD3+CD28 (green circles) and SEB (blue circles) stimulation systems, and discriminating protein analytes (q value [ANOVA FDR adjusted p value] < 0.05) were incorporated in the analysis. The PCA plot shown captures 90% of the total variance within the selected data set.

(B) The induced responses to whole-blood stimulations with CD3+CD28 and SEB were compared and the 12 differentially expressed proteins were identified (ANOVA q value < 0.05).

(C) The contribution of each protein analyte to the three principal component axes of the PCA plot are shown. (The positioning of the bars is arbitrary and is not considered negative or positive except in relation to the other analytes.)

(D) Correlation plots highlight differentially and similarly expressed proteins after whole-blood stimulations with CD3+CD28 (open green circles) or SEB (closed blue circles).

(E) Pairwise comparison for IL-6 and IL-4 concentration is shown after whole-blood stimulations with CD3+CD28 and SEB. Black lines indicate individual donors. Red star highlights non-responders to CD3+CD28 stimulation.

(F) The number of $CD3^+$ T cells per ml of whole blood in CD3+CD28-positive and -negative responders.

See also Figure S2.

concentrations of SEB-induced IL-6, IL-8, MCP-1, and IL-1β (Figure 3D). This was confirmed experimentally by intracellular flow cytometry staining, which showed that after SEB, but not CD3+CD28 stimulation, the MHCII-expressing monocytes were induced to express IL-8, MCP-1, and IL-1β protein (Figure S2). Interestingly, we observed that 6 of the 25 donors failed to produce IFN-γ, IL-2, IL-4, or IL-6 in response to CD3+CD28 stimulation, whereas all donors were capable of responding to SEB (Figures 3D and 3E). These data highlight the ability to reliably measure cell-cell interactions within the whole-blood stimulation conditions. Moreover, this approach permitted the identification of healthy donors that were unable to respond fully to anti-CD3 (clone UCHT1) stimulation, despite the binding of the antibody to donor T cells as confirmed by flow cytometry (Figure 3F).

Distinct Inflammatory Signatures Induced by Whole Microbes, Microbe-Associated Agonists, or Cytokine Stimulation

Complex stimuli used in our stimulation systems included heat-killed *Escherichia coli O111:B4* (HKEC), *Staphylococcus aureus* (HKSA), *Lactobacillus rhamnosus* (HKLR), *Helicobacter pylori* (HKHP), and *Candida albicans* (HKCA). Additionally, we utilized the clinical preparation of live bacillus Calmette-Guerin (BCG) and live stocks of H1N1 attenuated influenza A/PR8 (IAV) and Sendai virus (SeV) (Table 1). The *E. coli* used was derived from a strain that causes acute diarrhea in babies (Viljanen et al., 1990). *H. pylori* is also a human pathogen and is the main cause of ulcer disease and stomach cancer in humans (Wroblewski et al., 2010). Healthy donors may be carriers for *S. aureus* or *C. albicans*, but in some instances these agents may be the cause of human disease (e.g., in immunologically compromised individuals) (Gow et al., 2012; Otto, 2009). BCG is used as a vaccine in order to protect humans from childhood tuberculosis and is the standard of care for treatment of bladder cancer (NB: all donors received BCG vaccination) (Kawai et al., 2013; Romano and Huygen, 2012). *L. rhamnosus* is considered to be a transient inhabitant of humans and is present in some yogurt preparations (Borriello et al., 2003). Most humans are exposed to H1N1 IAV as a result of seasonal epidemics or through vaccination; and to serve as a contrast to IAV, we selected SeV, which does not infect humans yet triggers an innate inflammatory response (Kato et al., 2005; Norrby et al., 1992).

To characterize the patterns of protein analytes induced by such complex stimuli, we performed hierarchical clustering and

A

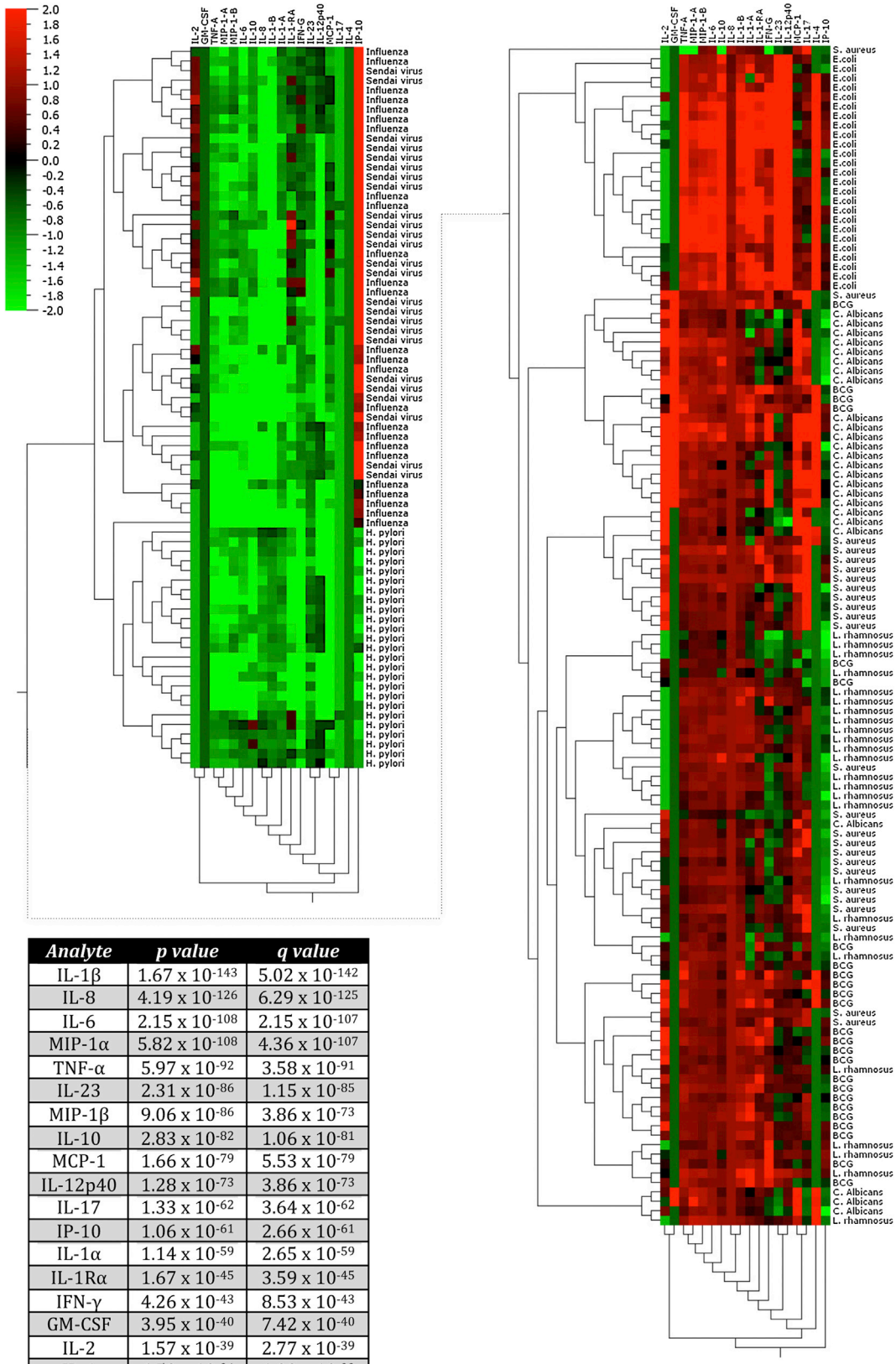

B

Analyte	*p value*	*q value*
IL-1β	1.67×10^{-143}	5.02×10^{-142}
IL-8	4.19×10^{-126}	6.29×10^{-125}
IL-6	2.15×10^{-108}	2.15×10^{-107}
MIP-1α	5.82×10^{-108}	4.36×10^{-107}
TNF-α	5.97×10^{-92}	3.58×10^{-91}
IL-23	2.31×10^{-86}	1.15×10^{-85}
MIP-1β	9.06×10^{-86}	3.86×10^{-73}
IL-10	2.83×10^{-82}	1.06×10^{-81}
MCP-1	1.66×10^{-79}	5.53×10^{-79}
IL-12p40	1.28×10^{-73}	3.86×10^{-73}
IL-17	1.33×10^{-62}	3.64×10^{-62}
IP-10	1.06×10^{-61}	2.66×10^{-61}
IL-1α	1.14×10^{-59}	2.65×10^{-59}
IL-1Rα	1.67×10^{-45}	3.59×10^{-45}
IFN-γ	4.26×10^{-43}	8.53×10^{-43}
GM-CSF	3.95×10^{-40}	7.42×10^{-40}
IL-2	1.57×10^{-39}	2.77×10^{-39}
IL-4	6.59×10^{-34}	1.09×10^{-33}

(legend on next page)

focused on the 18 most highly discriminating read-outs, all with a q value < 10^{-30} (Figures 4A and 4B). This approach separated IAV and SeV from the other stimuli, based on the induction of high IP-10 levels. HKEC was the most potent stimulus, marked by the highest levels of the pyrogenic cytokines TNF-α, IL-6, and IL-1β, as well as high levels of IL-12p40 and IL-23 (Figures 4A and S3). There was some overlap among the donor responses to HKCA, HKSA, HKLR, and BCG, but distinct patterns could be discerned. HKCA induced high amounts of GM-CSF in 20 of 25 donors, significantly higher than any other microbial stimulus (KW $p < 1 \times 10^{-7}$). As observed in the overall PCA plot (Figure 2), we could discriminate HKSA, BCG, and HKCA based on their induction of IL-2, possibly a reflection of our donor population having been previously exposed to these microbial agents (Figures 4A and S3). We also noted an interesting pattern of expression for IL-12p40, IL-12p70, and IL-23; most stimuli triggered IL-12p40, but only HKEC triggered IL-12p70 in a large number of donors (16 of 25) (Figure S3). Additionally, for some stimuli there appeared to be a bimodal pattern of induced responses, in particular the HKHP-, IAV-, and SeV-induced TNF-α and IL-12p40 and the HKEC-, HKLR-, HKCA-, IAV-, and SEV-induced IL-2 response (Figure S3).

We next selected the TLR agonists for analysis, because we achieved extensive coverage of this class of host sensors (Table 1). With the exception of the TLR1-TLR2 heterodimer, we were able to validate stimulation systems for the known TLR receptors expressed by humans (NB: Pam3CSK4 was evaluated, but failed short-term stability testing). FSL-1 (FSL, and also known as Pam2C) is a synthetic diacylated lipoprotein mimicking an agonist present in *Mycoplasma salivarium* (Okusawa et al., 2004). A high-molecular-weight, vaccine-grade poly IC (pIC) was used to activate TLR3. Ultrapure lipopolysaccharide (LPS) derived from *E. coli O111:B4* was used to stimulate TLR4. For TLR5, we selected ultrapure flagellin (FLA), extracted from *Salmonella* Typhimurium. To uniquely stimulate TLR7, we utilized the vaccine-grade preparation of Gardiquimod (GARD), an imidazoquinoline compound, and we used a related molecule, R848 (also vaccine-grade) as a stimulator with mixed agonist activity for TLR7 and TLR8. The TLR9 agonist selected was the class A CpG-2216 oligonucleotide (ODN), a fully synthetic oligonucleotide that contains unmethylated CpG dinucleotides within a particular sequence.

As shown in the PCA plot, it was possible to segregate the TLR stimuli based on the induced protein signatures. We selected the 11 most significant proteins (identified by ANOVA, q value < 10^{-60}), which allowed us to capture 93% of the measured variance in the response to TLR stimulation (Figure 5A). The notable exception was the overlap between FSL and FLA, which may be explained by the similar cellular expression of TLR2/6 and TLR5 on circulating monocytes (Mäkelä et al., 2009) and the use of a common MyD88-dependent signaling pathway (Takeda et al., 2003). R848 and GARD also showed a similar signature, yet the two could be segregated based on the overall higher levels of induced cytokines/chemokines and the increased number of donors that produced IL-12p70 to GARD (Figure S4A), a likely reflection of TLR8 engagement on monocytes (Bekeredjian-Ding et al., 2006). LPS triggered the strongest inflammatory response, as shown by the significantly higher levels of pyrogenic cytokines induced (TNF-α, IL-1β, and IL-6 higher for LPS as compared to the other stimuli, KW $p < 1 \times 10^{-7}$, Figure S4A). One caveat was a sampling bias in the selection of analytes measured, because the Luminex panels were oriented toward LPS-induced responses. We also highlight the relatively weak response induced by ODN, which we believe results from the agonist being quenched by the whole-blood matrix. Alternatively, it could be a reflection of the low numbers of plasmacytoid dendritic cells that are present within 1 ml of whole blood. However, upon removal of ODN from the analysis, the remaining TLR ligands kept their unique position (apart from FSL and FLA) within the PCA and a similar level of variance (94%) was captured (Figure S4B). In addition, we were able to distinguish ODN from the null condition based on eight analytes (ODN versus null, MW q < 0.05; Figures S4C and S4D), with the most induced protein being IP-10, a reflection of type I IFN being produced as a result of TLR9 stimulation (Krug et al., 2004). From the initial PCA plot (Figure 2), pIC stimulation could be distinguished by its unique inflammatory signature. This is recapitulated when pIC is compared to the other TLR agonists; the pattern of protein expression being remarkable for the high levels of IL-12p70 and the complete absence of induced IL-10. A bimodal distribution was again seen for some cytokines; in particular, a certain number of donors failed to produce IL-12p40 after FSL, FLA, or ODN and others did not produce IL-12p70 after LPS or R848 (Figure S4A).

To provide insight into the variable response to stimulation via cytokine receptors, we exposed cells to IFN-α_{2a}, IFN-β, IFN-γ, TNF-α, IL-1β, or IL-23. The latter four cytokines were also measured as one of the proteins assessed in the multiplex luninex assays. As such, we had an internal control that donors were stimulated with similar cytokine concentrations; additionally, it was important to exclude the measured variable from the stimulation signature (Figures S5). As expected because of their use of the same IFN-α/β receptor, the signatures for IFN-α_{2a} and IFN-β were identical and also similar to that seen for IFN-γ, which induces a common set of interferon-stimulated genes (ISGs) and proteins (Der et al., 1998). These data also permit deconvolution of some of the more complex signatures. For example, we highlight that pIC results in the induction of both TNF-α and IL-1β (Figure S4), both of which can induce IL-10 when they are used as stimuli (Figures S5); yet there was a clear absence of IL-10 induction upon pIC stimulation (Figure S4). Although this may be a reflection of lower levels

Figure 4. Unique Inflammatory Signatures Induced by Complex Microbial Stimulation

(A) Hierarchical clustering was performed on the data set obtained from 25 healthy donors, restricting the analysis to whole-blood stimulation by heat-killed (HK) *E. coli* (HKEC), HK *S. aureus* (HKSA), HK *L. rhamnosus* (HKLR), *bacillus Calmette-Guérin* (BCG), HK *H. pylori* (HKHP), HK *C. albicans* (HKCA), influenza A virus (IAV), and Sendai virus (SeV). A heat map is shown, based on the 18 most differentially induced proteins as defined by ANOVA q values.

(B) The 18 most differentially expressed proteins that were used to define microbe stimulation-specific signatures are listed in order of statistical significance (cutoff value was determined by ANOVA, q value < 10^{-30}).

See also Figure S3.

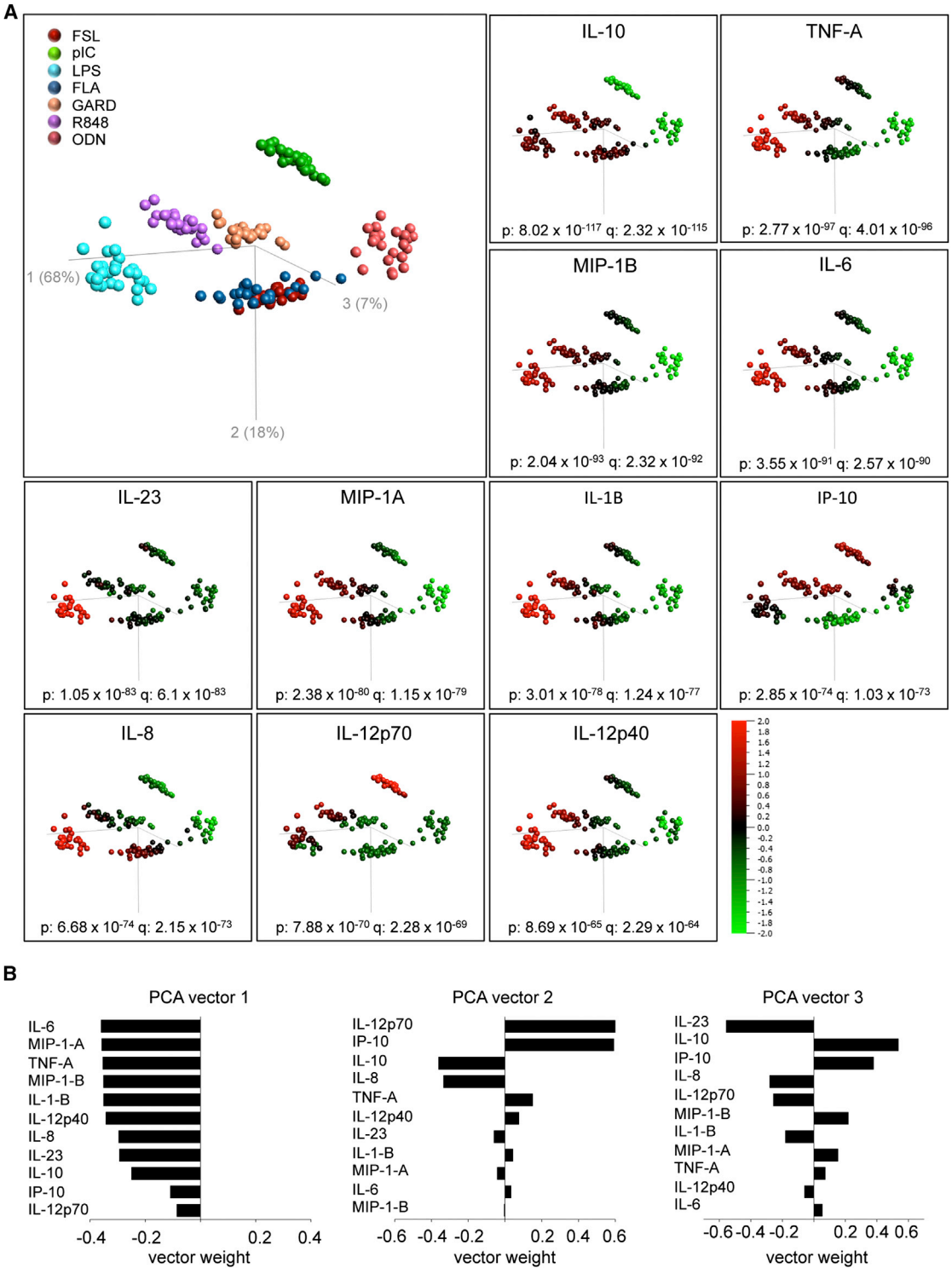

Figure 5. Segregation of TLR Agonists Based on Their Induced Protein Signatures

(A) Principal component analysis (PCA) was performed on the data set obtained from 25 healthy donors. Analysis was restricted to the 7 whole-blood stimulations that contained TLR agonists (FSL, pIC, LPS, FLA, GARD, R848, ODN). Each colored circle represents a different whole-blood stimulation condition, and the PCA was run with the 11 most differentially induced proteins (cutoff value was determined by ANOVA, q value < 10^{-60}). The PCA plot shown captures 85% of the total variance within the selected data set. Expression levels for each of the 11 protein analytes was overlaid on the PCA plot. A heat map indicates

(legend continued on next page)

of pIC-induced TNF-α and IL-1β, we favor the interpretation that TRIF activation or perhaps the high levels of STAT1 signaling results in suppression of IL-10 expression (Saraiva and O'Garra, 2010).

Characterization of Naturally Occurring Variance to Immune Stimulation

The development of reliable stimulation systems for monitoring immune responses permits the establishment of reference ranges for healthy individuals. Moreover, it permits the classification of inflammatory and host immune responses based on the variability among healthy donors as well as the identification of responses outside the defined reference range. To rapidly visualize variance among our 25 donors, we plotted the induced responses on a radar plot (Figure 6): absolute concentrations of the induced proteins are plotted along the spokes of the plot; lines trace the induced protein signature from individual donors; the shaded gray polygon indicates the median value of the null condition; and the black circles mark the induced fold change over the median null value. Data have been sorted so the least induced protein is at the top of the radar plot, with increasing fold change plotted in a clockwise manner. Analytes were excluded from the signature if the absolute value of the median fold change (stimulation/null) was <1.3. Data from the LPS stimulation system are shown and all plots can be found as an online Excel file (Document S2).

For the LPS-induced signature, we highlight that several induced cytokines and chemokines showed limited interindividual variance (CV < 50%). By contrast, other analytes showed high variance; for example, IL-12p70 and IFN-γ showed a range that spanned more than two orders of magnitude with CVs of 106% and 132%, respectively (Table S4). Additionally, this representation permitted the identification of two individuals that were outliers in their failure to produce measurable amounts of IL-1α in response to LPS (red star, Figure 6A). Notably, the rest of the signature was intact. To explore this finding further, we studied induced IL-1α across the entire stimulation space. Data from four consecutive donors are shown (including one of the outlier individuals identified), and we compared the response for three proteins that showed a high correlation (IL-1α, IL-1β, and IL-6). Expression of the IL-1 receptor antagonist (IL-1Ra) is also shown, because it is involved in the IL-1 pathway. Strikingly, none of the stimuli used triggered detectable levels of IL-1α production by donor 203 (or donor 312, not shown); this was in contrast to the induction of IL-1β and IL-6, which was within the range of values reported for the other donors tested (Figure 6B and Table S4). Given the importance of IL-1α in sterile inflammation and disease pathogenesis, we believe that our findings will be of general interest. Moreover, we highlight the value of utilizing standardized measures for host immune responses, thus enabling the identification of interindividual variance and extreme phenotypes among human populations.

DISCUSSION

The definition of host immune responses to microbial agents is of major interest and facilitates an increased understanding of human health and disease pathogenesis. Although functional tests are routinely used in laboratory investigation (Folds and Schmitz, 2003), the standardization of assays has been challenging. Indeed, there exist few examples of standardized systems for measuring induced immune response in human population-based studies or clinical practice. This study aimed at testing whole-blood stimulation systems for medically relevant stimuli to determine the inflammatory signature and characterize the naturally occurring variation present in a population of healthy donors of European descent. The robust definition of the boundaries of a healthy immune response at the population level is an indispensable prerequisite to subsequently understand how perturbations in these responses correlate and in some instances account for a pathologic state. Our approach utilizes a practical solution to monitoring induced immune responses and requires only 1 ml of blood per stimulation system and a 37°C heating block, maintained in room air. Additionally, there is minimal sample handling and specialized technical experience is not required.

The concept of utilizing whole-blood assays for assessing leukocyte function was first introduced by Ruuskanene and colleagues in 1975 (Eskola et al., 1975), used at that time for monitoring PHA and ConA-induced lymphocyte proliferation. Digel and colleagues extended this approach to the study of cytokines in 1983 (Digel et al., 1983), reporting the use of whole-blood stimulation with SEA and anti-CD3 antibodies, followed by the measurement of type I and type II interferons. Over the last three decades, whole-blood cultures have been utilized for probing various aspects of the immune response (Chen et al., 2010; De Groote et al., 1992; Ida et al., 2006; Kirchner et al., 1982; Nerad et al., 1992; Pott et al., 2009). However, several problems have persisted, including the ill-defined period of time between blood draw and cell culture and the requirements for specialized lab equipment (e.g., tissue culture hoods, CO_2 incubators). One notable exception has been the clinical development of the QuantiFERON TB Gold In-Tube (QFT-G IT) assay (Santin et al., 2012), which has been approved for the diagnosis of latent tuberculosis infection. QFT-G IT measures the induction of IFN-γ production in whole blood after in vitro stimulation with *Mycobacteria tuberculosis* antigens.

In this study, we report the development and testing of 27 stimulation systems, built into whole-blood syringes. We aimed to test our assay system via a broad array of immune stimuli, including bacteria, fungi, and viruses; agonists specific for defined innate immunity sensors; clinically employed cytokines; and activators of T cell immunity. With the exception of two assay systems (CPPD and WGP), the coefficient of variance was low, in the range of 5%–14%, with long-term stability of up to 12 months. The endpoints chosen for evaluating the

the relative expression of the indicated protein analyte (red indicating high levels of expression, green indicating low levels of expression). ANOVA p and q values are reported.
(B) The contribution of each protein analyte to the three principal component axes of the PCA plot are shown. (The positioning of the bars is arbitrary and is not considered negative or positive except in relation to the other analytes.)
See also Figure S4.

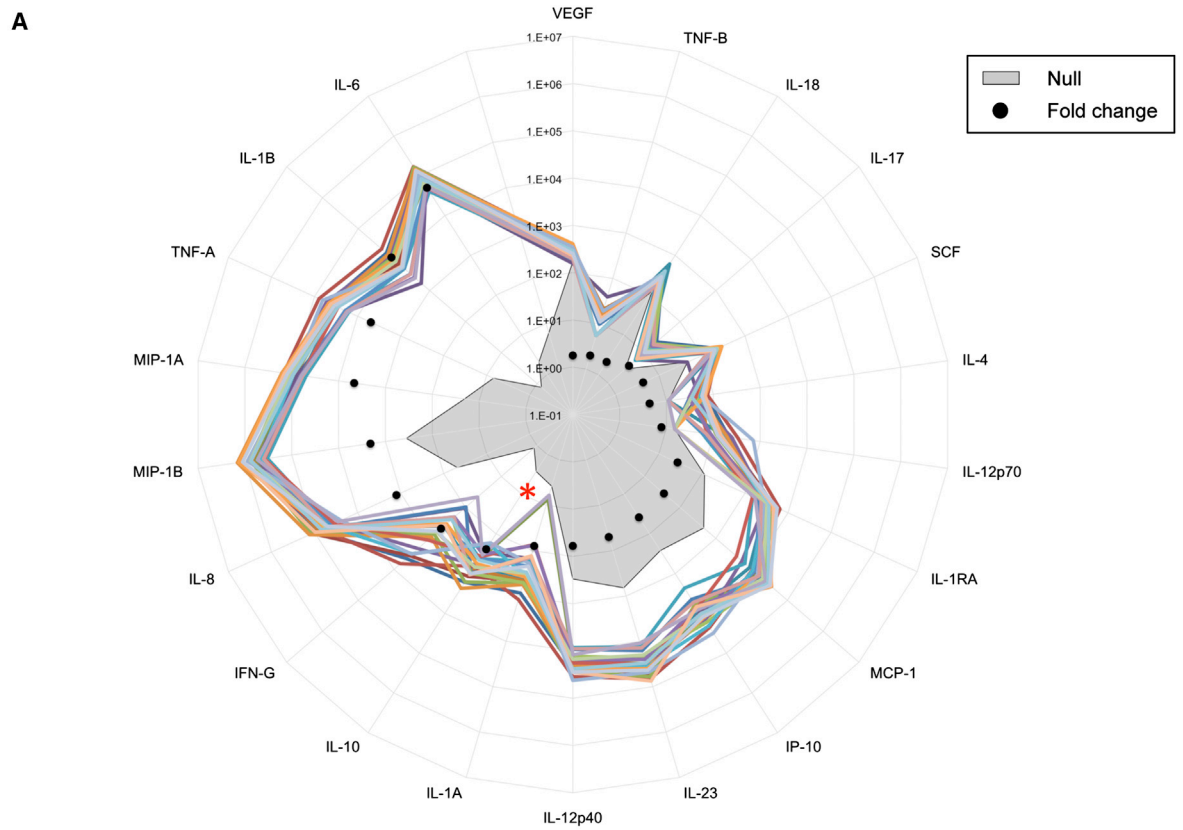

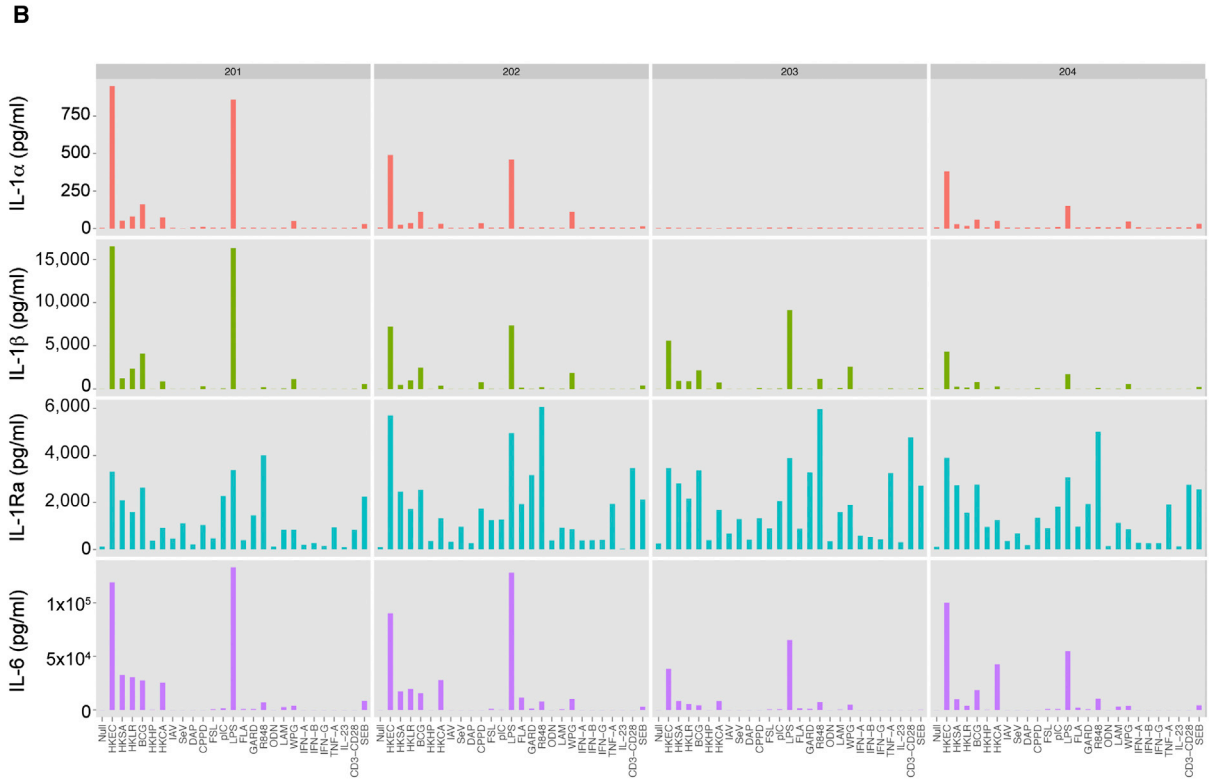

(legend on next page)

inflammatory signature consisted of a selection of inducible cytokines, chemokines, and growth factors. Importantly, dose-finding studies ensured that the induced responses did not exceed the biologic limit, as indicated by the broad range of analyte concentrations observed across the different stimulation conditions. Unique, specific signatures were identified for most stimulation systems. As an initial validation of lymphocyte activation, we observed an expected T cell signature (e.g., induction of IL-5, IL-2, GM-CSF, IL-4) when using anti-CD3 and anti-CD28 or SEB stimulation. These two signatures were clearly separated from the other stimuli in the global analysis and could be distinguished from each other, a result of SEB activation of MHCII-expressing cells. We also identified six healthy donors who failed to respond to CD3+CD28 stimulation despite binding of the CD3 antibody to T cells. This confirmed earlier reported findings and might be due to polymorphisms in the FcγRII expressed by monocytes (Ceuppens et al., 1985; Tax et al., 1983) that bind mouse IgG1 (the subclass of the UCHT-1 anti-CD3 clone used), or it might be due to other as yet unidentified common genetic variants. Interestingly, we also observed a modest "lymphocyte" signature when we utilized BCG, HKSA, and HKCA stimulation. Specifically, these three stimuli induced low levels of IL-2, which was not observed when we used HKEC, HKLR, or HKHP.

When directly comparing whole microbes, we could identify clear signatures for HKEC (strong induction of pyrogenic cytokines and high expression of both IL-12p70 and IL-23), HKCA (based on the stimulation of GM-CSF expression), and the two viral stimuli, IAV and SeV (triggering the highest levels of IP-10). Notably, the interindividual variance was highest for microbial-induced IL-2 and IFN-γ (CV in range of 78%–165%, 60%–183%, respectively), HKEC-induced IL-12p70 (CV = 155%), HKHP-induced IL-10 (CV = 216%), and BCG or HKCA-induced GM-CSF (CV = 175% and 216%, respectively). These differences are presumed to be due to a combination of host genetic factors and environmental, both internal and external, exposures (Newport et al., 2004). We may also consider that prior exposure and/or carrier state (e.g., colonization by HKCA) might account for differential memory responses (e.g., lymphocyte activation or antibody opsonization of the microbe) (Zielinski et al., 2012), in turn impacting the magnitude of the inflammatory response. We also highlight the relatively weak response to HKHP stimulation, which is probably due to the bacterium harboring an extensively modified lipid A moiety as part of its LPS, which reduces by >1,000-fold its TLR4 agonist activity (Cullen et al., 2011) and a flagellin that is poorly recognized by TLR5 (Gewirtz et al., 2004; Lee et al., 2003). Furthermore, stimulation of TLR2 by *H. pylori* mediates a tolerogenic response (Sun et al., 2013), potentially contributing to the weak response induced by HKHP.

To capture a more precise measure of the innate response, we also utilized purified or synthetic MAMPs known to engage the TLR, NLR, or CLR families of microbial sensors. These pathways have been heavily investigated over the past two decades and efforts are underway to establish some of the selected ligands as adjuvants for vaccine formulation. For NF-κB-induced cytokines (e.g., TNF-α, IL-1β, IL-6, MIP-1α, MIP-1β, IL-8, and IL-12p40), we found a similar pattern of expression across the different stimuli. LPS was unique in its induction of IL-23, whereas pIC induced the highest levels of IL-12p70. Although our *x*MAP testing did not evaluate many interferon-induced proteins, the levels of IP-10 were consistent with the endosomal TLRs being more robust stimulators of IRF3 than the surface receptors (Blasius and Beutler, 2010). DAP was a relatively weak stimulus, possibly because of poor membrane permeability, though we were able to observe a consistent induction of NF-κB-dependent chemokines or cytokines. Although they were less reliable than other stimulation systems, we were able to detect strong signatures by using CPPD and WGP, both of which showed high induction of IL-1β and measureable levels of IL-18, a likely result of inflammasome activation. Of note, the interindividual variance for many of the induced proteins was greater than the intraindividual variance of the assay systems. The LAM signature was notable for the highest interindividual variance in IL-10 among the different stimuli used (range 2.7–1,100 pg/ml; CV = 158% for LAM-induced IL-10). Our data are consistent with mRNA and protein expression patterns that have been evaluated via transcriptional profiling, ELISA, or Luminex on specific stimulated cell types, such as human monocytes and dendritic cells (Huang et al., 2001; Kwissa et al., 2012; Torri et al., 2010). Our study, however, represents a systematic evaluation of pattern recognition receptor (PRR) activation that takes into consideration the complex cellular interactions occurring in whole blood and serum matrix components, which might be closer to the natural conditions in which immune responses are provided.

One of the most interesting results of our study was the identification of 2 of 25 donors who did not release IL-1α after stimulation with any of the 27 different stimuli. Despite the failure to detect IL-1α, all remaining chemokine and cytokine signatures were intact for these donors, including the production of IL-1β. Two distinct but related genes, *IL1A* and *IL1B*, encode for IL-1α and IL-1β, respectively (Dinarello, 2009). Both bind the same surface receptor, and both are antagonized by the soluble protein IL-1Ra. Notably, IL-1 blockade, by means of IL-1RA or neutralizing antibodies, has become central to the clinical management of rheumatologic diseases and hereditary systemic autoinflammatory disorders (Dinarello et al., 2012). IL-1α is expressed by most cells and because of the lack of a signal peptide it is not readily secreted. Intracellular IL-1α is preformed

Figure 6. Interindividual Variance in the Response to LPS Stimulation

(A) Radar plot representation of the LPS-induced response obtained from 25 healthy donors. Analytes are represented as picograms per milliliter (pg/ml) and ordered clockwise in increasing fold change (as compared to null). Each donor is represented by a colored line, connecting the concentration of measured protein analytes. The gray polygon depicts the median value of the null response for the 25 donors. Black dots indicate the fold change as compared to the median value of the null response. Analytes with a median fold change (stimulation/null) >1.3 or <−1.3 were included. A red asterisk highlights the identification of two donors in which IL-1α was not induced above background.

(B) Histogram plots representing the IL-1α, IL-1β, IL-1Rα, and IL-6 response for 4 consecutive donors are shown for the Null condition and 26 whole-blood stimuli (NB: the IL-1β stimulation tube was omitted from analysis because it confounds the measurement of IL-1β).

See also Figure S5.

and bioactive; as such, its release from damaged cells is considered to be one of the first steps in the initiation of so-called sterile inflammation. In our study, we detected measurable amounts of IL-1α in the culture supernatant after whole-blood stimulation with HKEC, HKSA, HKLR, BCG, HKCA, SeV, CPPD, LPS, R848, and WPG (defined by median fold change over null stimulation > 1.3). Future studies will be required in order to identify how the genetic makeup of the host, including common polymorphisms in the European population, may account for the failure of the two donors to release IL-1α in the setting of multiple immune stimulations.

In summary, the whole-blood collection stimulation systems presented allow the definition of induced inflammatory signatures for a broad range of innate and adaptive stimuli, helping to address the urgent need for monitoring of functional immune responses in a reliable and reproducible manner. Moreover, we have identified preliminary boundaries for the natural variation in the induced immune protein phenotypes, setting the basis for a better understanding of the meaning of a healthy immune response. These tools will support integrative and systems-level human population-based studies (Braga-Neto and Marques, 2006) aimed at defining the genetic and/or environmental determinants of natural or disease-induced variation in immune responsiveness.

EXPERIMENTAL PROCEDURES

Donors

Samples were obtained as part of the *Milieur Intérieur* Healthy Donor Cohort. Details are provided in Supplemental Experimental Procedures and can found at http://www.clinicaltrials.gov (identifier NCT01699893).

Whole-Blood Stimulation

TruCulture tubes were prepared in batch with the indicated stimulus, resuspended in a volume of 2 ml buffered media, and maintained at −20°C until time of use. Blood was obtained from the antecubital vein by a 60 ml syringe containing sodium-heparin (50 IU/ml final concentration). Within 15 min of collection, 1 ml of whole blood was distributed into each of the prewarmed TruCulture tubes, inserted into a dry block incubator, and maintained at 37°C (±1°C) room air for 22 hr (±15 min). At the end of the incubation period, tubes were opened and a valve was inserted in order to separate the sedimented cells from the supernatant and to stop the stimulation reaction. Liquid supernatants were aliquoted and immediately frozen at −80°C until the time of use.

Multianalyte Profiling and Identification of Inflammatory Signatures

Supernatants from whole-blood stimulation systems were analyzed with Luminex *x*MAP technology. Samples were measured according to CLIA guidelines (validated by guidelines set forth by the USA Clinical and Laboratory Standards Institute). The 32 measured analytes were organized on three multiplex arrays, and a single batch of reagents was used for testing all samples. The least detectable dose (LDD) for each assay was derived by averaging the values obtained from 200 runs with the matrix diluent and adding 3 standard deviations to the mean. The lower limit of quantification (LLOQ) is determined based on the standard curve for each assay and is the lowest concentration of an analyte in a sample that can be reliably detected and at which the total error meets CLIA requirements for laboratory accuracy. For analytes tested, the LDD and LLOQ can be found in Table S3. The lower assay limit (LAL) is the lowest value read out after application of the standard curve and use of curve-fitting algorithms. In most instances, the LAL is less than the LDD and the LLOQ. For data mining, individual values below the LAL were replaced with a value that is 50% of the lowest value measured in the data set.

Statistical Analysis and Data Visualization

Principal component analysis (PCA), agglomerative hierarchical clustering, and ANOVA testing were performed with Qlucore Omics Explorer, v.2.3 (Qlucore). We report ANOVA-based p values, and to correct for multiple testing we report false discovery rate (FDR)-adjusted ANOVA p values, called q values. Dot plot graphs and two-way correlation plots were compiled with GraphPad Prism v.6.0. Correlation matrices and bar graphs were calculated with R v.2.15.1 and drawn with graphical package ggplot2 v.0.9.3.

SUPPLEMENTAL INFORMATION

Supplemental Information includes Supplemental Experimental Procedures, five figures, four tables, and one data set and can be found with this article online at http://dx.doi.org/10.1016/j.immuni.2014.03.002.

CONSORTIA

Milieu Intérieur Consortium team leaders: Laurent Abel, Andres Alcover, Philippe Bousso, Ana Cumano, Marc Daëron, Cécile Delval, Caroline Demangel, Ludovic Deriano, James Di Santo, Françoise Dromer, Gérard Eberl, Jost Enninga, Antonio Freitas, Ivo G. Boneca, Serge Hercberg, Olivier Lantz, Claude Leclerc, Hugo Mouquet, Sandra Pellegrini, Stanislas Pol, Lars Rogge, Anavaj Sakuntabhai, Olivier Schwartz, Benno Schwikowski, Spencer Shorte, Vassili Soumelis, Frédéric Tangy, Eric Tartour, Antoine Toubert, Marie-Noëlle Ungeheuer, Lluis Quintana-Murci, and Matthew L. Albert. Additional information can be found at http://www.milieuinterieur.fr/en.

ACKNOWLEDGMENTS

This work benefited from support of the French government's Invest in the Future Program, managed by the Agence Nationale de la Recherche (ANR, reference 10-LABX-69-01). We also acknowledge A. Pugsley for his support in obtaining funding and the logistical aspects of initiating the project.

Received: July 11, 2013
Accepted: January 15, 2014
Published: March 20, 2014

REFERENCES

Alexopoulou, L., Holt, A.C., Medzhitov, R., and Flavell, R.A. (2001). Recognition of double-stranded RNA and activation of NF-kappaB by Toll-like receptor 3. Nature *413*, 732–738.

Allen, I.C., Scull, M.A., Moore, C.B., Holl, E.K., McElvania-TeKippe, E., Taxman, D.J., Guthrie, E.H., Pickles, R.J., and Ting, J.P. (2009). The NLRP3 inflammasome mediates in vivo innate immunity to influenza A virus through recognition of viral RNA. Immunity *30*, 556–565.

Andersson, A., Olofsson, T., Lindgren, D., Nilsson, B., Ritz, C., Edén, P., Lassen, C., Råde, J., Fontes, M., Mörse, H., et al. (2005). Molecular signatures in childhood acute leukemia and their correlations to expression patterns in normal hematopoietic subpopulations. Proc. Natl. Acad. Sci. USA *102*, 19069–19074.

Bekeredjian-Ding, I., Roth, S.I., Gilles, S., Giese, T., Ablasser, A., Hornung, V., Endres, S., and Hartmann, G. (2006). T cell-independent, TLR-induced IL-12p70 production in primary human monocytes. J. Immunol. *176*, 7438–7446.

Blasius, A.L., and Beutler, B. (2010). Intracellular toll-like receptors. Immunity *32*, 305–315.

Borriello, S.P., Hammes, W.P., Holzapfel, W., Marteau, P., Schrezenmeir, J., Vaara, M., and Valtonen, V. (2003). Safety of probiotics that contain lactobacilli or bifidobacteria. Clin. Infect. Dis. *36*, 775–780.

Braga-Neto, U.M., and Marques, E.T., Jr. (2006). From functional genomics to functional immunomics: new challenges, old problems, big rewards. PLoS Comput. Biol. *2*, e81.

Brown, G.D., Herre, J., Williams, D.L., Willment, J.A., Marshall, A.S., and Gordon, S. (2003). Dectin-1 mediates the biological effects of beta-glucans. J. Exp. Med. *197*, 1119–1124.

Ceuppens, J.L., Meurs, L., and Van Wauwe, J.P. (1985). Failure of OKT3 monoclonal antibody to induce lymphocyte mitogenesis: a familial defect in monocyte helper function. J. Immunol. *134*, 1498–1502.

Chamaillard, M., Hashimoto, M., Horie, Y., Masumoto, J., Qiu, S., Saab, L., Ogura, Y., Kawasaki, A., Fukase, K., Kusumoto, S., et al. (2003). An essential role for NOD1 in host recognition of bacterial peptidoglycan containing diaminopimelic acid. Nat. Immunol. *4*, 702–707.

Chen, J., Bruns, A.H., Donnelly, H.K., and Wunderink, R.G. (2010). Comparative in vitro stimulation with lipopolysaccharide to study TNFalpha gene expression in fresh whole blood, fresh and frozen peripheral blood mononuclear cells. J. Immunol. Methods *357*, 33–37.

Cullen, T.W., Giles, D.K., Wolf, L.N., Ecobichon, C., Boneca, I.G., and Trent, M.S. (2011). *Helicobacter pylori* versus the host: remodeling of the bacterial outer membrane is required for survival in the gastric mucosa. PLoS Pathog. *7*, e1002454.

De Groote, D., Zangerle, P.F., Gevaert, Y., Fassotte, M.F., Beguin, Y., Noizat-Pirenne, F., Pirenne, J., Gathy, R., Lopez, M., Dehart, I., et al. (1992). Direct stimulation of cytokines (IL-1 beta, TNF-alpha, IL-6, IL-2, IFN-gamma and GM-CSF) in whole blood. I. Comparison with isolated PBMC stimulation. Cytokine *4*, 239–248.

Der, S.D., Zhou, A., Williams, B.R., and Silverman, R.H. (1998). Identification of genes differentially regulated by interferon alpha, beta, or gamma using oligonucleotide arrays. Proc. Natl. Acad. Sci. USA *95*, 15623–15628.

Diebold, S.S., Kaisho, T., Hemmi, H., Akira, S., and Reis e Sousa, C. (2004). Innate antiviral responses by means of TLR7-mediated recognition of single-stranded RNA. Science *303*, 1529–1531.

Digel, W., Marcucci, F., and Kirchner, H. (1983). Induction of interferon gamma in leucocyte cultures of the peripheral blood of mice. J. Interferon Res. *3*, 65–69.

Dinarello, C.A. (2009). Immunological and inflammatory functions of the interleukin-1 family. Annu. Rev. Immunol. *27*, 519–550.

Dinarello, C.A. (2012). Keep up the heat on IL-1. Blood *120*, 2538–2539.

Dinarello, C.A., Simon, A., and van der Meer, J.W. (2012). Treating inflammation by blocking interleukin-1 in a broad spectrum of diseases. Nat. Rev. Drug Discov. *11*, 633–652.

Eskola, J., Soppi, E., Viljanen, M., and Ruuskanen, O. (1975). A new micromethod for lymphocyte stimulation using whole blood. Immunol. Commun. *4*, 297–307.

Fleischer, B., and Schrezenmeier, H. (1988). T cell stimulation by staphylococcal enterotoxins. Clonally variable response and requirement for major histocompatibility complex class II molecules on accessory or target cells. J. Exp. Med. *167*, 1697–1707.

Folds, J.D., and Schmitz, J.L. (2003). 24. Clinical and laboratory assessment of immunity. J. Allergy Clin. Immunol. Suppl. *111*, S702–S711.

Gantner, B.N., Simmons, R.M., Canavera, S.J., Akira, S., and Underhill, D.M. (2003). Collaborative induction of inflammatory responses by dectin-1 and Toll-like receptor 2. J. Exp. Med. *197*, 1107–1117.

Gewirtz, A.T., Yu, Y., Krishna, U.S., Israel, D.A., Lyons, S.L., and Peek, R.M., Jr. (2004). *Helicobacter pylori* flagellin evades toll-like receptor 5-mediated innate immunity. J. Infect. Dis. *189*, 1914–1920.

Godaly, G., and Young, D.B. (2005). *Mycobacterium bovis* bacille Calmette Guerin infection of human neutrophils induces CXCL8 secretion by MyD88-dependent TLR2 and TLR4 activation. Cell. Microbiol. *7*, 591–601.

González-Navajas, J.M., Lee, J., David, M., and Raz, E. (2012). Immunomodulatory functions of type I interferons. Nat. Rev. Immunol. *12*, 125–135.

Goodridge, H.S., Reyes, C.N., Becker, C.A., Katsumoto, T.R., Ma, J., Wolf, A.J., Bose, N., Chan, A.S., Magee, A.S., Danielson, M.E., et al. (2011). Activation of the innate immune receptor Dectin-1 upon formation of a 'phagocytic synapse'. Nature *472*, 471–475.

Gow, N.A., van de Veerdonk, F.L., Brown, A.J., and Netea, M.G. (2012). *Candida albicans* morphogenesis and host defence: discriminating invasion from colonization. Nat. Rev. Microbiol. *10*, 112–122.

Hayashi, F., Smith, K.D., Ozinsky, A., Hawn, T.R., Yi, E.C., Goodlett, D.R., Eng, J.K., Akira, S., Underhill, D.M., and Aderem, A. (2001). The innate immune response to bacterial flagellin is mediated by Toll-like receptor 5. Nature *410*, 1099–1103.

Hemmi, H., Takeuchi, O., Kawai, T., Kaisho, T., Sato, S., Sanjo, H., Matsumoto, M., Hoshino, K., Wagner, H., Takeda, K., and Akira, S. (2000). A Toll-like receptor recognizes bacterial DNA. Nature *408*, 740–745.

Hemmi, H., Kaisho, T., Takeuchi, O., Sato, S., Sanjo, H., Hoshino, K., Horiuchi, T., Tomizawa, H., Takeda, K., and Akira, S. (2002). Small anti-viral compounds activate immune cells via the TLR7 MyD88-dependent signaling pathway. Nat. Immunol. *3*, 196–200.

Huang, Q., Liu, D., Majewski, P., Schulte, L.C., Korn, J.M., Young, R.A., Lander, E.S., and Hacohen, N. (2001). The plasticity of dendritic cell responses to pathogens and their components. Science *294*, 870–875.

Ichinohe, T., Lee, H.K., Ogura, Y., Flavell, R., and Iwasaki, A. (2009). Inflammasome recognition of influenza virus is essential for adaptive immune responses. J. Exp. Med. *206*, 79–87.

Ida, J.A., Shrestha, N., Desai, S., Pahwa, S., Hanekom, W.A., and Haslett, P.A. (2006). A whole blood assay to assess peripheral blood dendritic cell function in response to Toll-like receptor stimulation. J. Immunol. Methods *310*, 86–99.

Józefowski, S., Sobota, A., Pawłowski, A., and Kwiatkowska, K. (2011). Mycobacterium tuberculosis lipoarabinomannan enhances LPS-induced TNF-α production and inhibits NO secretion by engaging scavenger receptors. Microb. Pathog. *50*, 350–359.

Jurk, M., Heil, F., Vollmer, J., Schetter, C., Krieg, A.M., Wagner, H., Lipford, G., and Bauer, S. (2002). Human TLR7 or TLR8 independently confer responsiveness to the antiviral compound R-848. Nat. Immunol. *3*, 499.

Kato, H., Sato, S., Yoneyama, M., Yamamoto, M., Uematsu, S., Matsui, K., Tsujimura, T., Takeda, K., Fujita, T., Takeuchi, O., and Akira, S. (2005). Cell type-specific involvement of RIG-I in antiviral response. Immunity *23*, 19–28.

Kato, H., Takeuchi, O., Sato, S., Yoneyama, M., Yamamoto, M., Matsui, K., Uematsu, S., Jung, A., Kawai, T., Ishii, K.J., et al. (2006). Differential roles of MDA5 and RIG-I helicases in the recognition of RNA viruses. Nature *441*, 101–105.

Kawai, K., Miyazaki, J., Joraku, A., Nishiyama, H., and Akaza, H. (2013). Bacillus Calmette-Guerin (BCG) immunotherapy for bladder cancer: current understanding and perspectives on engineered BCG vaccine. Cancer Sci. *104*, 22–27.

Kirchner, H., Kleinicke, C., and Digel, W. (1982). A whole-blood technique for testing production of human interferon by leukocytes. J. Immunol. Methods *48*, 213–219.

Kolb, W.P., and Granger, G.A. (1968). Lymphocyte in vitro cytotoxicity: characterization of human lymphotoxin. Proc. Natl. Acad. Sci. USA *61*, 1250–1255.

Krieg, A.M. (2002). CpG motifs in bacterial DNA and their immune effects. Annu. Rev. Immunol. *20*, 709–760.

Krishna, S., and Miller, L.S. (2012). Host-pathogen interactions between the skin and *Staphylococcus aureus*. Curr. Opin. Microbiol. *15*, 28–35.

Krug, A., Luker, G.D., Barchet, W., Leib, D.A., Akira, S., and Colonna, M. (2004). Herpes simplex virus type 1 activates murine natural interferon-producing cells through toll-like receptor 9. Blood *103*, 1433–1437.

Kwissa, M., Nakaya, H.I., Oluoch, H., and Pulendran, B. (2012). Distinct TLR adjuvants differentially stimulate systemic and local innate immune responses in nonhuman primates. Blood *119*, 2044–2055.

Lee, S.K., Stack, A., Katzowitsch, E., Aizawa, S.I., Suerbaum, S., and Josenhans, C. (2003). *Helicobacter pylori* flagellins have very low intrinsic activity to stimulate human gastric epithelial cells via TLR5. Microbes Infect. *5*, 1345–1356.

Liu-Bryan, R., Pritzker, K., Firestein, G.S., and Terkeltaub, R. (2005). TLR2 signaling in chondrocytes drives calcium pyrophosphate dihydrate and monosodium urate crystal-induced nitric oxide generation. J. Immunol. *174*, 5016–5023.

Maecker, H.T., McCoy, J.P., and Nussenblatt, R. (2012). Standardizing immunophenotyping for the Human Immunology Project. Nat. Rev. Immunol. *12*, 191–200.

Mäkelä, S.M., Strengell, M., Pietilä, T.E., Osterlund, P., and Julkunen, I. (2009). Multiple signaling pathways contribute to synergistic TLR ligand-dependent cytokine gene expression in human monocyte-derived macrophages and dendritic cells. J. Leukoc. Biol. *85*, 664–672.

March, C.J., Mosley, B., Larsen, A., Cerretti, D.P., Braedt, G., Price, V., Gillis, S., Henney, C.S., Kronheim, S.R., Grabstein, K., et al. (1985). Cloning, sequence and expression of two distinct human interleukin-1 complementary DNAs. Nature *315*, 641–647.

Martinon, F., Pétrilli, V., Mayor, A., Tardivel, A., and Tschopp, J. (2006). Gout-associated uric acid crystals activate the NALP3 inflammasome. Nature *440*, 237–241.

Means, T.K., Wang, S., Lien, E., Yoshimura, A., Golenbock, D.T., and Fenton, M.J. (1999). Human toll-like receptors mediate cellular activation by Mycobacterium tuberculosis. J. Immunol. *163*, 3920–3927.

Miettinen, M., Veckman, V., Latvala, S., Sareneva, T., Matikainen, S., and Julkunen, I. (2008). Live *Lactobacillus rhamnosus* and *Streptococcus pyogenes* differentially regulate Toll-like receptor (TLR) gene expression in human primary macrophages. J. Leukoc. Biol. *84*, 1092–1100.

Nerad, J.L., Griffiths, J.K., Van der Meer, J.W., Endres, S., Poutsiaka, D.D., Keusch, G.T., Bennish, M., Salam, M.A., Dinarello, C.A., and Cannon, J.G. (1992). Interleukin-1 beta (IL-1 beta), IL-1 receptor antagonist, and TNF alpha production in whole blood. J. Leukoc. Biol. *52*, 687–692.

Newport, M.J., Goetghebuer, T., Weiss, H.A., Whittle, H., Siegrist, C.A., and Marchant, A.; MRC Gambia Twin Study Group (2004). Genetic regulation of immune responses to vaccines in early life. Genes Immun. *5*, 122–129.

Norrby, E., Kövamees, J., Blixenkrone-Möller, M., Sharma, B., and Orvell, C. (1992). Humanized animal viruses with special reference to the primate adaptation of morbillivirus. Vet. Microbiol. *33*, 275–286.

Okusawa, T., Fujita, M., Nakamura, J., Into, T., Yasuda, M., Yoshimura, A., Hara, Y., Hasebe, A., Golenbock, D.T., Morita, M., et al. (2004). Relationship between structures and biological activities of mycoplasmal diacylated lipopeptides and their recognition by toll-like receptors 2 and 6. Infect. Immun. *72*, 1657–1665.

Oppmann, B., Lesley, R., Blom, B., Timans, J.C., Xu, Y., Hunte, B., Vega, F., Yu, N., Wang, J., Singh, K., et al. (2000). Novel p19 protein engages IL-12p40 to form a cytokine, IL-23, with biological activities similar as well as distinct from IL-12. Immunity *13*, 715–725.

Otto, M. (2009). *Staphylococcus epidermidis*—the 'accidental' pathogen. Nat. Rev. Microbiol. *7*, 555–567.

Platanias, L.C. (2005). Mechanisms of type-I- and type-II-interferon-mediated signalling. Nat. Rev. Immunol. *5*, 375–386.

Poltorak, A., He, X., Smirnova, I., Liu, M.Y., Van Huffel, C., Du, X., Birdwell, D., Alejos, E., Silva, M., Galanos, C., et al. (1998). Defective LPS signaling in C3H/HeJ and C57BL/10ScCr mice: mutations in Tlr4 gene. Science *282*, 2085–2088.

Pott, G.B., Chan, E.D., Dinarello, C.A., and Shapiro, L. (2009). Alpha-1-antitrypsin is an endogenous inhibitor of proinflammatory cytokine production in whole blood. J. Leukoc. Biol. *85*, 886–895.

Randhawa, A.K., Shey, M.S., Keyser, A., Peixoto, B., Wells, R.D., de Kock, M., Lerumo, L., Hughes, J., Hussey, G., Hawkridge, A., et al.; South African Tuberculosis Vaccine Initiative Team (2011). Association of human TLR1 and TLR6 deficiency with altered immune responses to BCG vaccination in South African infants. PLoS Pathog. *7*, e1002174.

Romano, M., and Huygen, K. (2012). An update on vaccines for tuberculosis - there is more to it than just waning of BCG efficacy with time. Expert Opin. Biol. Ther. *12*, 1601–1610.

Santin, M., Muñoz, L., and Rigau, D. (2012). Interferon-γ release assays for the diagnosis of tuberculosis and tuberculosis infection in HIV-infected adults: a systematic review and meta-analysis. PLoS ONE *7*, e32482.

Saraiva, M., and O'Garra, A. (2010). The regulation of IL-10 production by immune cells. Nat. Rev. Immunol. *10*, 170–181.

Schmolz, M., Hurst, T.L., Bailey, D.M., Powell, J.R., Forsey, R.J., Thompson, J.M., Williams, C., and Pawelec, G. (2004). Validation of a new highly standardised, lab-independent whole-blood leukocyte function assay for clinical trials (ILCS). Exp. Gerontol. *39*, 667–671.

Shibata, K., Hasebe, A., Sasaki, T., and Watanabe, T. (1997). Mycoplasma salivarium induces interleukin-6 and interleukin-8 in human gingival fibroblasts. FEMS Immunol. Med. Microbiol. *19*, 275–283.

Shimazu, R., Akashi, S., Ogata, H., Nagai, Y., Fukudome, K., Miyake, K., and Kimoto, M. (1999). MD-2, a molecule that confers lipopolysaccharide responsiveness on Toll-like receptor 4. J. Exp. Med. *189*, 1777–1782.

Sieling, P.A., Chatterjee, D., Porcelli, S.A., Prigozy, T.I., Mazzaccaro, R.J., Soriano, T., Bloom, B.R., Brenner, M.B., Kronenberg, M., Brennan, P.J., et al. (1995). CD1-restricted T cell recognition of microbial lipoglycan antigens. Science *269*, 227–230.

Smith-Garvin, J.E., Koretzky, G.A., and Jordan, M.S. (2009). T cell activation. Annu. Rev. Immunol. *27*, 591–619.

Stuyt, R.J., Netea, M.G., Kim, S.H., Novick, D., Rubinstein, M., Kullberg, B.J., Van der Meer, J.W., and Dinarello, C.A. (2001). Differential roles of interleukin-18 (IL-18) and IL12 for induction of gamma interferon by staphylococcal cell wall components and superantigens. Infect. Immun. *69*, 5025–5030.

Stuyt, R.J., Kim, S.H., Reznikov, L.L., Fantuzzi, G., Novick, D., Rubinstein, M., Kullberg, B.J., van der Meer, J.W., Dinarello, C.A., and Netea, M.G. (2003). Regulation of *Staphylococcus epidermidis*-induced IFN-gamma in whole human blood: the role of endogenous IL-18, IL-12, IL-1, and TNF. Cytokine *21*, 65–73.

Sun, X., Zhang, M., El-Zataari, M., Owyang, S.Y., Eaton, K.A., Liu, M., Chang, Y.M., Zou, W., and Kao, J.Y. (2013). TLR2 mediates *Helicobacter pylori*-induced tolerogenic immune response in mice. PLoS ONE *8*, e74595.

Takeda, K., Kaisho, T., and Akira, S. (2003). Toll-like receptors. Annu. Rev. Immunol. *21*, 335–376.

Takeuchi, O., Hoshino, K., Kawai, T., Sanjo, H., Takada, H., Ogawa, T., Takeda, K., and Akira, S. (1999). Differential roles of TLR2 and TLR4 in recognition of gram-negative and gram-positive bacterial cell wall components. Immunity *11*, 443–451.

Tax, W.J., Willems, H.W., Reekers, P.P., Capel, P.J., and Koene, R.A. (1983). Polymorphism in mitogenic effect of IgG1 monoclonal antibodies against T3 antigen on human T cells. Nature *304*, 445–447.

Torri, A., Beretta, O., Ranghetti, A., Granucci, F., Ricciardi-Castagnoli, P., and Foti, M. (2010). Gene expression profiles identify inflammatory signatures in dendritic cells. PLoS ONE *5*, e9404.

Viljanen, M.K., Peltola, T., Junnila, S.Y., Olkkonen, L., Järvinen, H., Kuistila, M., and Huovinen, P. (1990). Outbreak of diarrhoea due to *Escherichia coli O111:B4* in schoolchildren and adults: association of Vi antigen-like reactivity. Lancet *336*, 831–834.

Wroblewski, L.E., Peek, R.M., Jr., and Wilson, K.T. (2010). *Helicobacter pylori* and gastric cancer: factors that modulate disease risk. Clin. Microbiol. Rev. *23*, 713–739.

Yoneyama, M., Kikuchi, M., Matsumoto, K., Imaizumi, T., Miyagishi, M., Taira, K., Foy, E., Loo, Y.M., Gale, M., Jr., Akira, S., et al. (2005). Shared and unique functions of the DExD/H-box helicases RIG-I, MDA5, and LGP2 in antiviral innate immunity. J. Immunol. *175*, 2851–2858.

Zhao, Y., Yokota, K., Ayada, K., Yamamoto, Y., Okada, T., Shen, L., and Oguma, K. (2007). *Helicobacter pylori* heat-shock protein 60 induces interleukin-8 via a Toll-like receptor (TLR)2 and mitogen-activated protein (MAP) kinase pathway in human monocytes. J. Med. Microbiol. *56*, 154–164.

Zheng, Y., Humphry, M., Maguire, J.J., Bennett, M.R., and Clarke, M.C. (2013). Intracellular interleukin-1 receptor 2 binding prevents cleavage and activity of interleukin-1α, controlling necrosis-induced sterile inflammation. Immunity *38*, 285–295.

Zielinski, C.E., Mele, F., Aschenbrenner, D., Jarrossay, D., Ronchi, F., Gattorno, M., Monticelli, S., Lanzavecchia, A., and Sallusto, F. (2012). Pathogen-induced human TH17 cells produce IFN-γ or IL-10 and are regulated by IL-1β. Nature *484*, 514–518.